

Article

Mechanical Properties of 3D-Printed Components Using Fused Deposition Modeling: Optimization Using the Desirability Approach and Machine Learning Regressor

Vijaykumar S. Jatti , Mandar S. Sapre *, Ashwini V. Jatti, Nitin K. Khedkar and Vinaykumar S. Jatti *

Symbiosis Institute of Technology, Symbiosis International (Deemed) University, Pune 412115, Maharashtra, India
* Correspondence: mandar.sapre@sitpune.edu.in (M.S.S.); vinayjatti@sitpune.edu.in (V.S.J.)

Abstract: The fused deposition modelling (FDM) technique involves the deposition of a fused layer of material according to the geometry designed in the software. Several parameters affect the quality of parts produced by FDM. This paper investigates the effect of FDM printing process parameters on tensile strength, impact strength, and flexural strength. The effects of process parameters such as printing speed, layer thickness, extrusion temperature, and infill percentage are studied. Polyactic acid (PLA) was used as a filament material for printing test specimens. The experimental layout is designed according to response surface methodology (RSM) and responses are collected. Specimens are prepared for testing of these parameters as per ASTM standards. A mathematical model for each of the responses is developed based on the nonlinear regression method. The desirability approach, nonlinear regression, as well as experimental values are in close agreement with each other. The desirability approach predicted the tensile strength, impact strength, and flexural strength with a less percentage error of 3.109, 6.532, and 3.712, respectively. The nonlinear regression approach predicted the tensile strength, impact strength, and flexural strength with a less percentage error of 2.977, 6.532, and 3.474, respectively. The desirability concept and nonlinear regression approach resulted in the best mechanical property of the FDM-printed part.



Citation: Jatti, V.S.; Sapre, M.S.; Jatti, A.V.; Khedkar, N.K.; Jatti, V.S. Mechanical Properties of 3D-Printed Components Using Fused Deposition Modeling: Optimization Using the Desirability Approach and Machine Learning Regressor. *Appl. Syst. Innov.* **2022**, *5*, 112. <https://doi.org/10.3390/asi5060112>

Received: 19 September 2022

Accepted: 1 November 2022

Published: 7 November 2022

Publisher's Note: MDPI stays neutral with regard to jurisdictional claims in published maps and institutional affiliations.



Copyright: © 2022 by the authors. Licensee MDPI, Basel, Switzerland. This article is an open access article distributed under the terms and conditions of the Creative Commons Attribution (CC BY) license (<https://creativecommons.org/licenses/by/4.0/>).

Keywords: nonlinear regression; fused deposition modeling; desirability concept; design of experiments; response surface methodology

1. Introduction

Fused deposition modelling is an additive manufacturing technology in which the mechanical and surface properties obtained should be comparable to those of the conventional injection moulding process [1–4]. Numerous studies have been conducted to study the effect of process parameters on the fused deposition modelling parts' mechanical and surface properties. Kantaros et al. [5] examined the effect of layer thickness and deposition orientation on the magnitude of the solidification-induced residual strains. Further, the specimens were subjected to a thermal cycle. The developed residual strains and coefficient of thermal expansion of the ABS parts were measured using an optical sensor with a short fiber Bragg grating. Sood et al. [6] utilized Taguchi's experimental layout to investigate the effect of layer thickness, part orientation, raster angle, air gap, and raster width on the part dimensional accuracy in terms of the percentage change in length, width, and thickness during 3D printing of ABSP400. Artificial neural network was employed for the prediction of dimensional accuracy. Sood et al. [7] employed a central composite design to investigate the influence of air gap, raster width, raster angle, part orientation, and layer thickness on impact, flexural, and tensile strength. Distortion between or within layers resulted in lower strength of the parts. Es-Said et al. [8] developed the ABS parts using a Stratasys machine for five-layer orientations. The parts' impact resistance, modulus of rupture, and tensile strength were observed, and it was found that, at 0 degrees, orientation layers deposited along the length of samples showed better considered mechanical properties than other orientations. Fragile interlayer bonding and porosity may result in the anisotropic properties. Kantaros et al. [9]

discussed the 3D printing challenges faced by the users of a low-cost desktop 3D printer. The illustrated the means of addressing these challenges by tuning selected process parameters to obtain the best print quality. Vasudevarao et al. [10] designed an experimental layout using fractional factorial design with two levels for each factor to estimate the optimal surface finish by obtaining optimal parameter settings of layer thickness, air gap, build orientation, and road width. Kantaros et al. [11] demonstrated the effect of bead orientation and air gap on the developed residual strains in prismatic specimens built using fused deposition modeling. Residual strains are measured using an optical sensor with a short fiber Bragg grating.

The literature suggests that 3D-printed parts have at least 30% worse mechanical behaviour than injection-moulded parts. The process parameters are scattered over a large range, which results in the best mechanical and surface properties. This requires significant experimentation to identify the influencing parameters. Different optimization techniques were employed by researchers, namely, response surface methodology, Taguchi method, full factorial design, fractional factorial design, grey relation analysis, artificial neural network, fuzzy logic, genetic algorithm, and so on, to improve the mechanical properties of parts by optimizing a number of FDM process parameters [12–17]. Selecting a part for an application requires the forecasting of how the part will perform under different loading conditions. Hence, it is becoming essential to study the effect of FDM process parameters on mechanical properties. The literature depicts that various studies have been carried out using different types of materials and settings of process parameters. Table 1 provides a summary of the literature survey in terms of process parameters, filament material, output parameters, methods adopted for experimentation and optimization, and key findings.

Table 1. Summary of the literature review.

Reference No.	Input Process Parameters	Filament Material	Method/Technique	Output Parameters
[18]	Infill density, infill pattern, print speed, and print temperature	PLA, ABS, CFR-PLA, CFR-ABS, CNT-ABS	One-variable-at-a-time	Tensile, compressive, flexural
[19]	Infill density and angle of orientation	PLA	Full factorial	Tensile
[20]	Raster angle	PLA	One-variable-at-a-time	Tensile, fracture
[21]	Layer thickness, raster width, airgap, and part orientation	PLA, ABS	Response surface methodology	Geometrical deformation, surface roughness
[22]	Raster angle, raster width, and layer height	PLA	Adaptive neuro-fuzzy interface system	Tensile
[23]	Infill density, speed, and print temperature	PLA	Central composite design, genetic algorithm, adaptive neuro-fuzzy interface system, artificial neural network	Tensile
[24]	Infill density, print speed, and layer thickness	PLA	Taguchi method	Tensile
[25]	Infill density, layer thickness, and extrusion temperature	PLA	Taguchi method	Tensile, impact, and hardness
[26]	Layer height, shell thickness, infill density, orientation angle, and print speed	PLA	Taguchi method	Tensile
[27]	Layer thickness, airgap, orientation, temperature	PLA	One-variable-at-a-time, chemical treatment	Tensile
[28]	Infill density	PLA	Full factorial	Tensile, hardness, impact, flexural
[29]	Build direction, infill percentage, and layer thickness	CFR-PLA	The technique for order of preference by similarity to ideal solution	Tensile, izod impact
[30]	Layer thickness, nozzle temperature, bed temperature, infill density	PLA	One-variable-at-a-time	Tensile
[31]	Infill density, print speed, and layer height	CFR-PLA	Taguchi	Tensile
[32]	Print orientation, bed temperature, nozzle temperature, print speed, infill density	CFR-PLA	Taguchi	Tensile, impact
[33]	Infill density and print pattern	PLA	Taguchi	Tensile
[34]	Infill density and infill pattern	PLA, ABS, PETG	Full factorial	Tensile
[35]	Print speed and print temperature	PLA	Full factorial	Tensile
[36]	Print orientation and layer thickness	PLA	Full factorial	Tensile
[37]	Infill density number of aluminum layer and bed temperature	PLA	Taguchi method	Tensile
[38]	Layer height, infill percentage, and infill pattern	PLA	Central composite design	Tensile
[39]	Layer thickness, print orientation	PLA	Generalized-relative root-mean-square error	Tensile
[40]	Layer height, fill density, printing velocity, and orientation	PLA	Taguchi method	Tensile
[41]	Raster angle and moisture content	PLA	Design of experiments	Tensile, strain, modulus of elasticity
[42]	Layer height, extrusion width, printing temperature, printing speed	FR-PLA	Central composite design	Tensile
[43]	Bed temperature, extrusion temperature	PLA, CF-PLA	Central composite design	Tensile, flexural, shear

Awasthi and Banerjee [44] presented a review on methods to 3D print thermoplastic materials. They depicted the strategies to overcome defects in 3D printing of thermoplastic elastomers, enhancing the mechanical and thermoplastic elastomeric properties of 3D-printed parts. They identified the scope for future work and motivation to enhance the research in this field. The authors summarized the research carried out to date on thermoplastic elastomeric material, which can act as a guideline to academics and the industry. Cuan-Urquizo et al. [45] presented a review on experimental, computational, and theoretical approaches with regard to fused filament fabrication parts' mechanical properties. The authors depicted the applications and limitations of each of these approaches. At the end, they provided future directions for characterizing printed materials and areas that require further research. Verma et al. [46] studied the influence of styrene/isoprene/styrene, bed temperature, print temperature, layer thickness, print speed, infill density, and the number of shells on the mechanical properties and printability using the Taguchi method. The authors claimed that their study resulted in less voids in the printed parts and improved the adhesion between phases.

The main objective of this study was to achieve the optimal settings of 3D printer process parameters to obtain enhanced tensile, impact, and flexural strength of the printed components using PLA filament material. The scope of this study includes the design of experimentation as per central composite design with 31 runs. The three responses considered as parameters for the study are tensile, impact, and flexural strength. The test specimens for tensile, impact, and flexural strength are prepared as per ASTM D638, ASTM D256, and ASTM D790, respectively. The mathematical model for predicting tensile, impact, and flexural strength was developed according to a machine learning non-linear regression approach. Optimization of the input parameters was performed using a desirability approach and non-linear regression approach. Further validation experiments were carried out to confirm the optimized values obtained from the nonlinear regression approach and desirability concept.

The paper is organized into Section 2 presenting the materials and methods, Section 3 presenting the results and discussion, and Section 4 presenting the conclusions with future work.

2. Materials and Methods

The FDM process involves the following steps. A CAD model is generated and then converted into STL files for stereolithography. Three-dimensional surfaces are represented in this file as an assembly of planar triangles. The greater the number of triangles, the better the accuracy. Once the STL file has been converted, the slicing process involves steps including describing the 3D part, dividing the parts into slices, and determining the support material and path as well as the angle of the tool. Various parameters are set in the STL file to specify how the machines will operate in the various layers. The FDM samples are created using a Creality Ender 3 machine with a bed size of $220 \times 220 \times 250 \text{ mm}^3$. CATIA software is used to design the parts. It is then converted into an STL file, which is sliced into machine-readable g-code files using the Cura engine of the Repetier software. The dimensions of the tensile specimen are $63.5 \times 9.53 \times 3.2 \text{ mm}^3$, which are as per the ASTM D638 requirements. The impact specimen dimensions are $63 \times 12.7 \times 3.2 \text{ mm}^3$, follow the ASTM D256 requirements. The dimensions of the flexural specimen are $125 \times 12.7 \times 3.2 \text{ mm}^3$, which are as per the ASTM D790 requirements. The dimensions are shown in Figure 1. The material used to create the specimen is polylactic acid (PLA), which is commonly used for FDM-processed parts. The tensile strength of the specimens is determined using the uniaxial tensile tests.

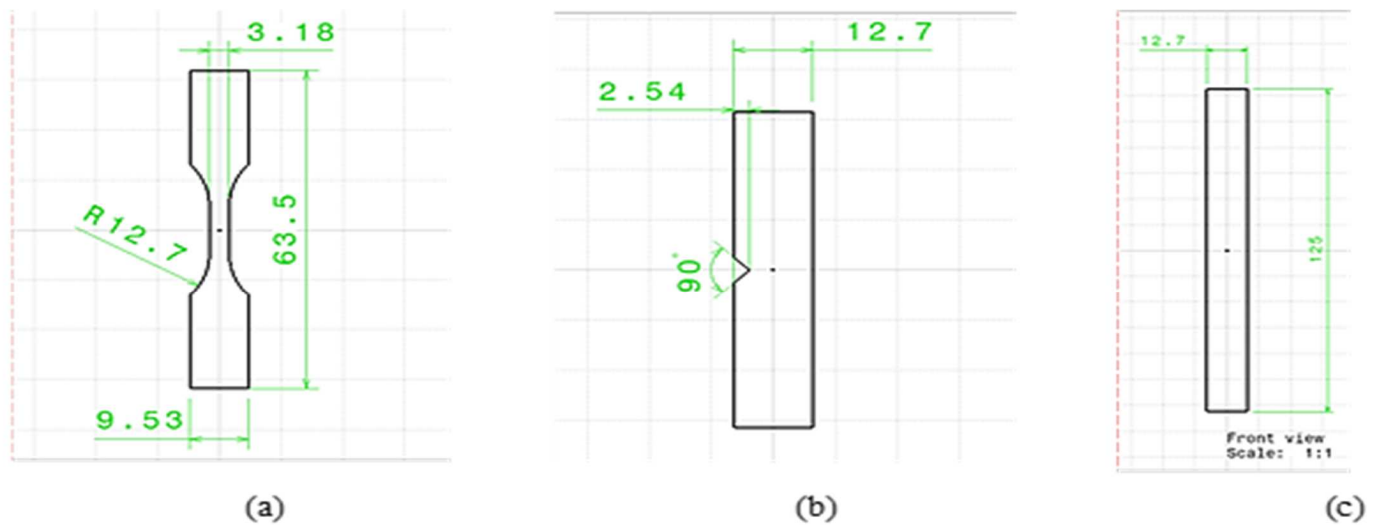


Figure 1. Dimensions of the (a) tensile specimen, (b) impact specimen, and (c) flexural specimen.

The three main aspects of DOE are factors, levels, and response. The term level indicates the number of different values a variable can assume according to its discretization. Design matrices are used, which have tables that have all of the combinations of levels between the different factors. The DOE factors considered in these experiments are as follows:

1. **Infill Percentage**—The infill percentage measures the amount of material inside the fabricated part. It represents the density of the part. The infill percentage is set according to the part's requirement. The values for the infill percentage are chosen as 10, 33, 55, 78, and 100%.
2. **Layer Thickness**—In FDM, the thickness of a single layer deposited by the nozzle is the layer thickness. The type of nozzle used decides the paper thickness. The nozzle diameter used in this case is 0.4 mm. The values for the layer height are chosen as 0.08 mm, 0.16 mm, 0.24 mm, 0.32 mm, and 0.4 mm.
3. **Print Speed**—The speed of the nozzle with which the material will be deposited is denoted as the print speed. A very high printing speed will cause the wear and tear of physical parts and lead to improper distribution of materials. Moreover, a low printing speed is not suitable as it will increase the time required to print one specimen. Hence, the values for print speed are set as 20, 35, 50, 65, and 80 mm/s.
4. **Extrusion Temperature**—The extrusion temperature is the temperature at which the material is extruded from the nozzle. The extruder contains a heater that heats the material up to a semi-liquid state. As the temperature increases, the viscosity of the material increases. As a result, it is necessary to set the extruder temperature within the limits where semi-liquid materials can be kept. The capacity of the heating system decides the temperatures at which materials are extruded. Temperatures are set at 190, 200, 210, 220, and 230 °C.

Table 2 depicts the experimental runs and observed values of responses. Tensile test specimens were prepared as per ASTM D638 standard, flexural test specimens were prepared as per ASTM D790 standard, and impact test specimens were prepared as per ASTM D256. Tensile and flexural test was conducted on UTM of VEEKAY TESTLAB and the impact test was conducted on an impact testing machine of ADVANCE EQUIPMENTS having a least count of 0.0001 J. Figure 2a–c shows the setup of the tensile, flexural, and impact test. Figure 2d–f shows the actual test piece after the performance of tests.



(a)



(b)

Figure 2. Cont.

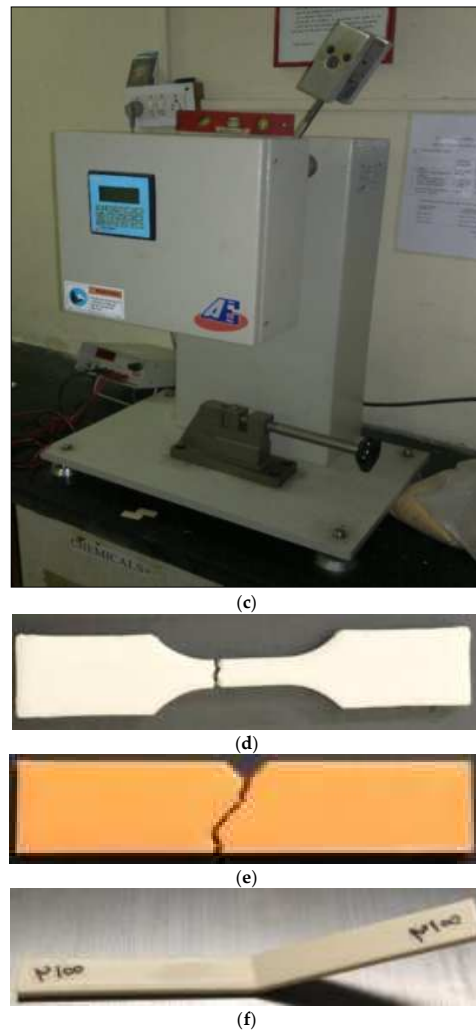


Figure 2. (a) Tensile test setup, (b) flexural test setup, (c) impact test setup, (d) tensile test piece after test, (e) impact test piece after test, (f) flexural test piece after test.

Table 2. Input and output parameters.

Run Nos.	Infill Percentage	Layer Height (mm)	Print Speed (mm/s)	Extrusion Temp (°C)	Tensile Strength (N/mm ²)	Impact Strength (kJ/m ²)	Flexural Strength (N/mm ²)
1	78	0.32	35	220	46.17	1.55	39.07
2	10.5	0.24	50	210	42.78	1.59	51.01
3	33	0.16	35	220	45.87	3.2	43.13
4	33	0.32	35	200	41.18	3.32	30.9
5	33	0.16	65	200	43.59	3.31	37.8
6	100.5	0.24	50	210	54.20	3.37	62.51
7	78	0.16	35	200	51.88	3.31	53.06
8	33	0.32	65	200	43.19	3.25	44.74
9	78	0.32	65	200	50.34	3.31	48.2
10	33	0.16	65	220	45.72	3.27	42.79
11	78	0.16	35	220	53.35	3.35	52.27
12	55.5	0.24	50	210	49.67	3.22	53.93
13	33	0.32	35	220	45.08	3.3	42.88
14	55.5	0.24	50	190	47.56	3.37	48.38
15	55.5	0.24	50	210	48.39	3.38	51.15
16	78	0.32	65	220	46.49	3.2	56.59
17	55.5	0.24	50	210	47.21	3.38	50.53
18	55.5	0.24	50	210	48.30	3.36	62.67
19	55.5	0.24	50	230	50.15	1.71	52.21
20	33	0.32	65	220	43.35	3.32	40.58
21	55.5	0.24	50	210	45.33	3.47	53
22	55.5	0.24	80	210	45.56	3.38	52.18
23	78	0.16	65	200	49.84	3.35	50.73
24	55.5	0.24	20	210	48.51	3.52	39.54
25	55.5	0.08	50	210	42.63	3.37	44.21
26	55.5	0.4	50	210	42.87	3.17	45.64
27	55.5	0.24	50	210	47.14	3.47	46.05
28	78	0.32	35	200	45.17	3.41	60.88
29	55.5	0.24	50	210	47.07	3.43	55.67
30	78	0.16	65	220	50.99	3.2	57.67
31	33	0.16	35	200	43.75	3.35	42.55

3. Results and Discussion

In this study, a total of 31 experiments were carried out as per the response surface methodology and a detailed study on all of these results, such as the effect of process parameters on the tensile strength, flexural strength, and impact strength, is discussed below. The graphs for the same are shown below in Figures 3–5, respectively.

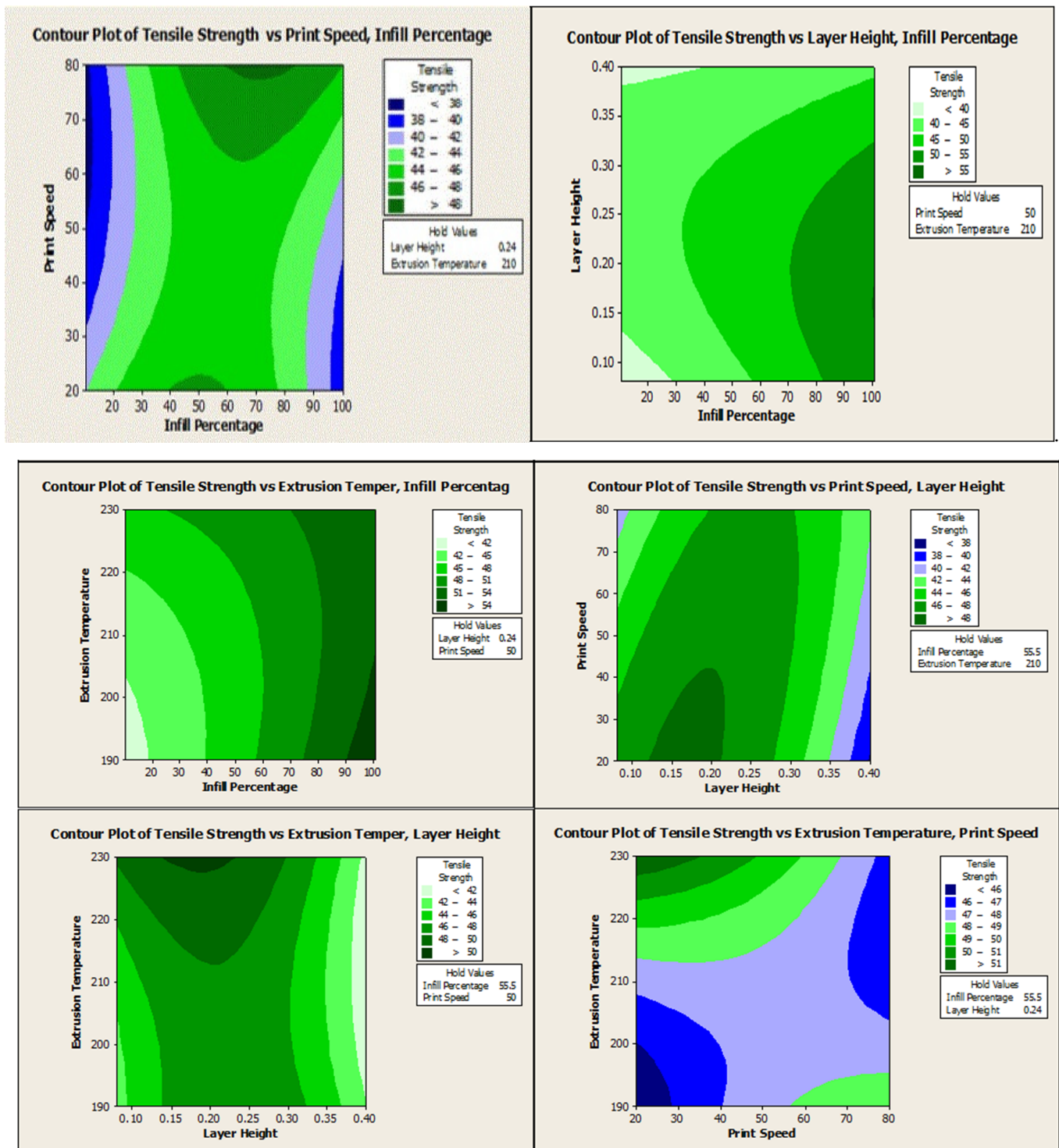


Figure 3. Effect of process parameters on the tensile strength.

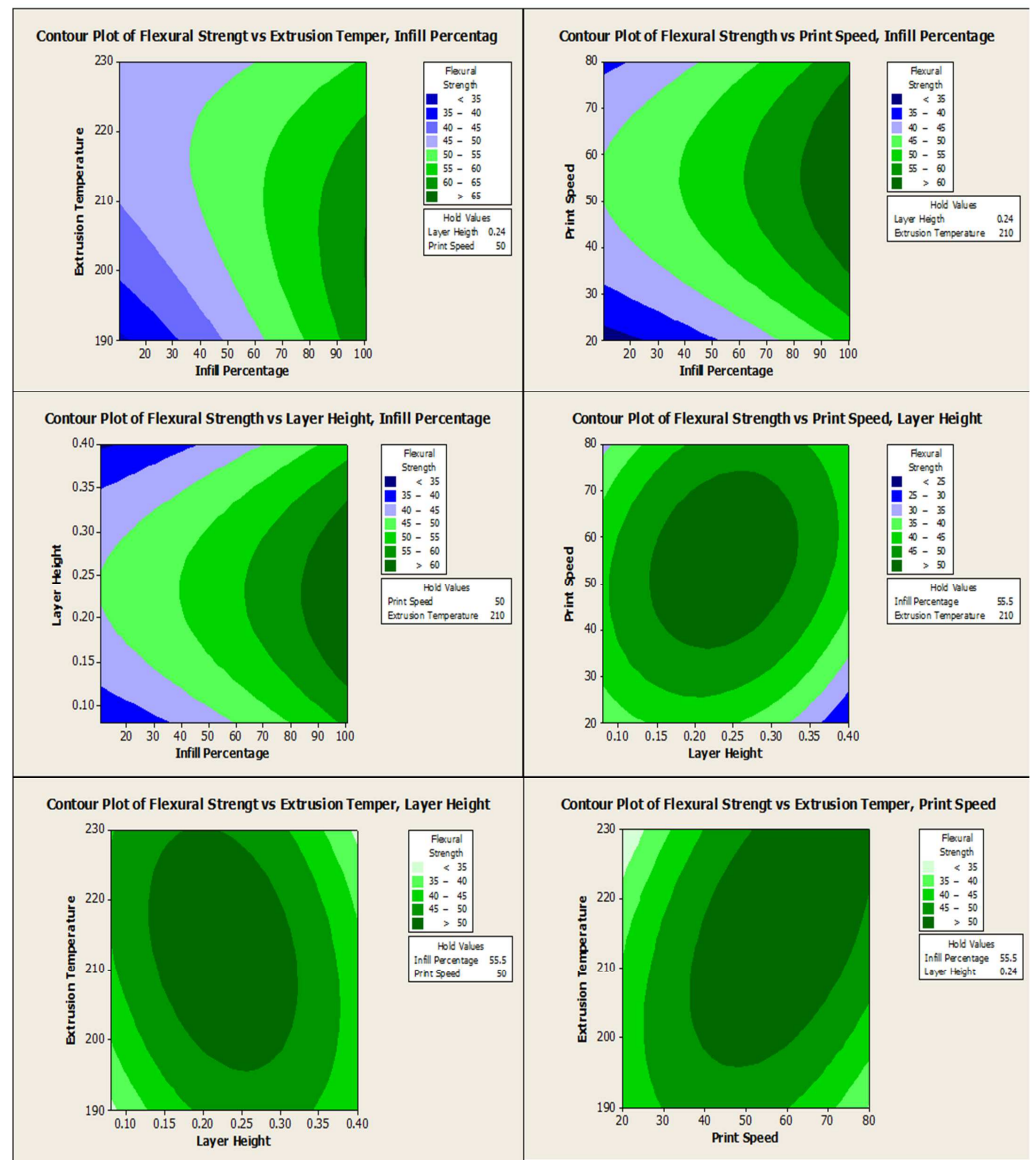


Figure 4. Effect of process parameters on the flexural strength.

3.1. Analysis Using Desirability Approach

Using a computerized uniaxial tensile testing machine in accordance with ASTM D638 standards, the mechanical behavior of the parts was investigated. When the specimen breaks under the load, as in tensile testing, the breaking load is noted on the digital screen. From Figure 3, it can be understood that the tensile strength increases with the increase in infill percentage. A greater infill percentage implies a higher density of the part. This will increase the strength required for pulling and breaking the specimen. Hence, the tensile strength will increase. In the extrusion process, the nozzle temperature causes the material to melt into a semi-liquid phase. The material tends to shift slightly towards a liquid state when the extrusion temperature is increased, resulting in reduced viscosity. The less viscous material is now in an oval shape and not circular. The contact area between layers is enlarged as the brittleness of the material is increased with an increase in temperature. Moreover, one can expect that the material becomes more brittle with a larger temperature increase. Thus, larger contact areas tend to increase strength, but the increase is very minimal. As the infill filament has had less time to cool down between each passage, the adhesion between the filaments in a faster-printed object is better. Thus, the filament's maximum strength may be slightly improved. Owing to the unevenness of the material

deposit, the overall strength of the fabricated part can be reduced at high speeds. Therefore, the strength increases through adhesion are cancelled out and the tensile strength remains almost constant as the printing speed changes. If the layer height is increased, the tensile strength of the part will decrease. As a result of fewer layers, the printed part has less adhesion and accuracy, which significantly decreases its tensile strength.

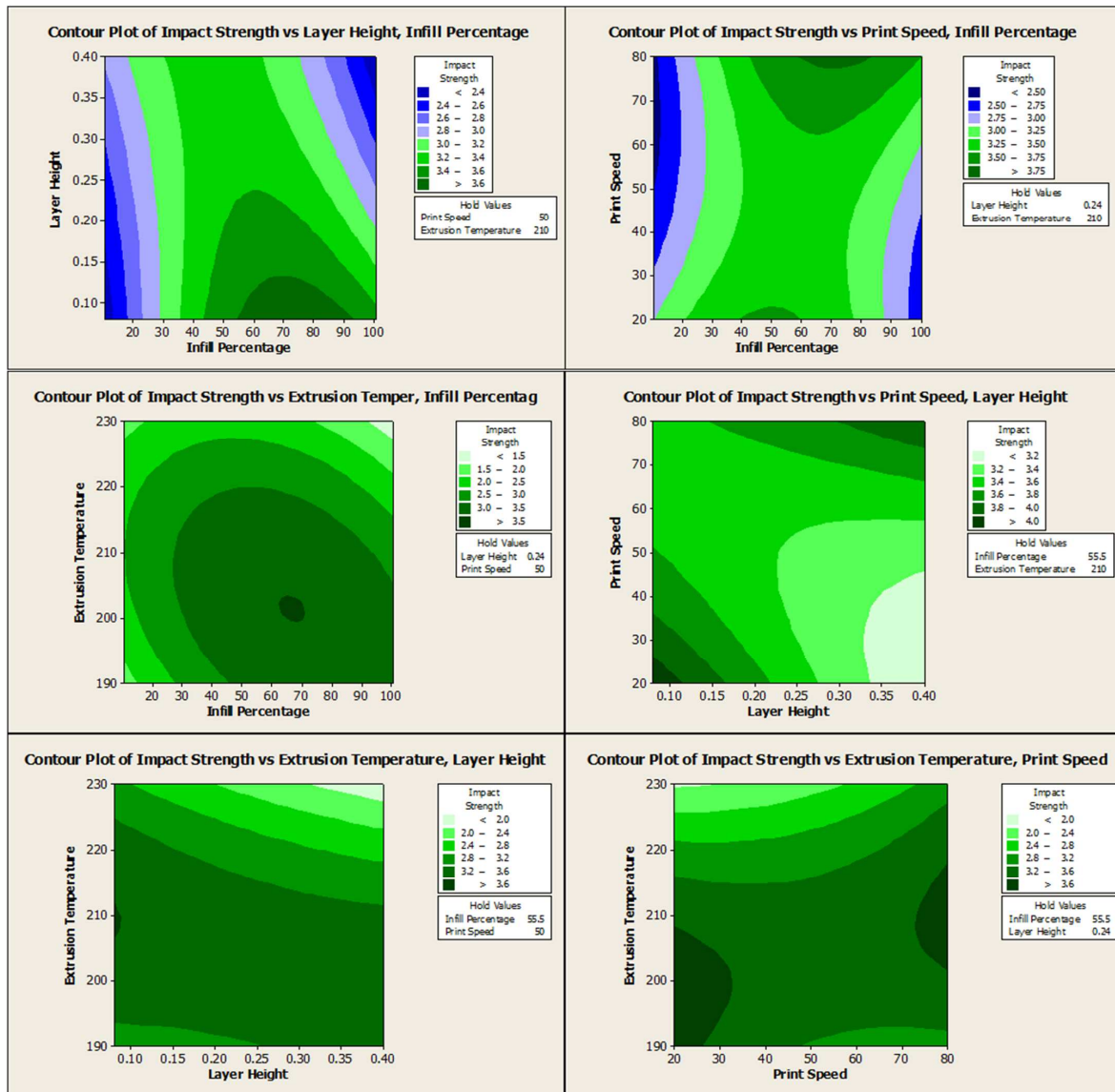
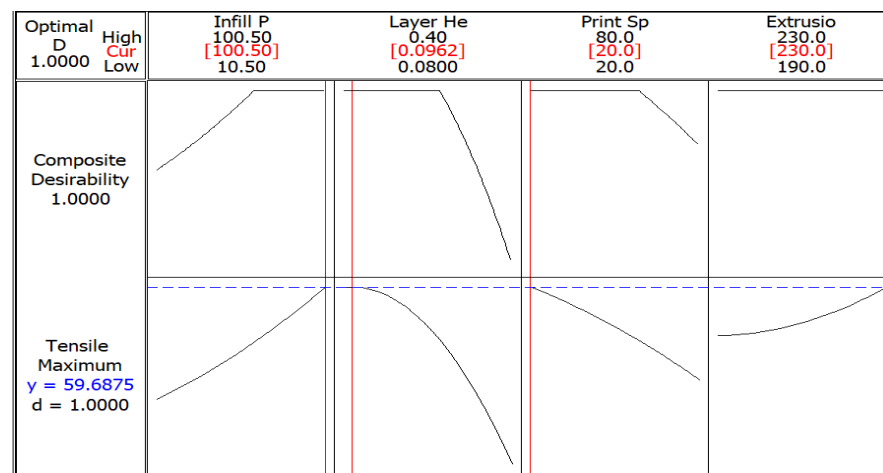


Figure 5. Effect of process parameters on the impact strength.

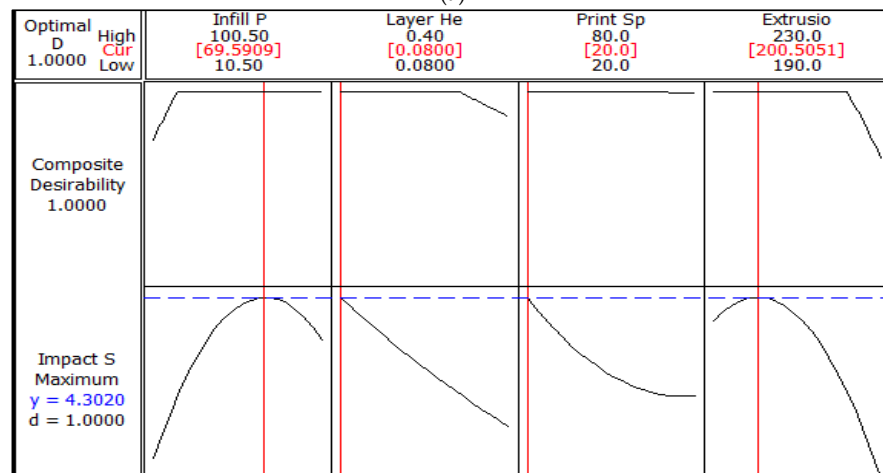
Flexural strength indicates the amount of bending it can withstand. Flexural strength increases with the increase in infill percentage, layer height, and extrusion temperature, while it decreases slightly with the increase in print speed. Owing to a lower infill percentage, there is less density in the fabricated part. Owing to more hollow space inside the part, there are no proper supports from the inside, hence the part is weaker. For this reason, the part is easily broken upon bending. An increase in infill percentage strengthens the part, thus increasing the flexural strength. However, we have seen that a change in the combination of different parameters actually increases the properties more than just changing one parameter at a time. The above graphs show us that maximum flexural strength can be obtained with a lower value of extrusion temperature, while simultaneously setting a higher value of the infill percentage.

Impact strength is the toughness of the part, which in turn indicates its ability to absorb energy during plastic deformation. Figure 5 shows that the impact strength of the FDM-printed parts is affected by every parameter. Impact strength increases with an increase in infill percentage, layer height, and print speed, while it decreases considerably with an increase in extrusion temperature. Based on our study, there was a significant relationship between the apparent density and the impact absorption capacity, both of which were measured for the components in terms of dissipation of energy. However, the result of layer height was less significant. As discussed earlier, the rise in extrusion temperature reduces the viscosity, which in turn decreases the layer thickness slightly. The dimensional accuracy of the part is affected. There is a decrease in the thickness of the fabricated part and less impact energy is required to cause the failure of the part. Thus, as the extrusion temperature increases, the impact strength decreases.

From Figure 6, the infill percentage, layer height, print speed, and extrusion temperature should be 100%, 0.0962 mm, 20 mm/s, and 230 °C, respectively, to obtain the optimum tensile strength. The optimum impact strength can be obtained if the infill percentage, layer height, print speed, and extrusion temperature are 70%, 0.08 mm, 20 mm/s, and 201 °C, respectively. To obtain optimum the flexural strength, the infill percentage, layer height, print speed, and extrusion temperature should be set at 100%, 0.24 mm, 52 mm/s, and 203 °C, respectively. Similarly, to obtain the optimum surface roughness, the infill percentage, layer height, print speed, and extrusion temperature should be 43%, 0.14 mm, 45 mm/s, and 230 °C, respectively.



(a)



(b)

Figure 6. Cont.

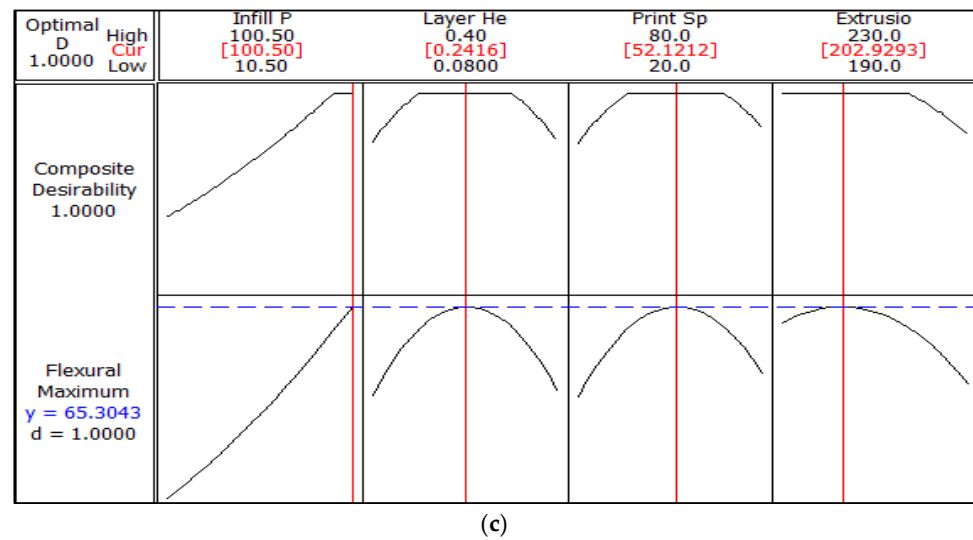


Figure 6. (a) Desirability optimization for tensile strength, (b) desirability optimization for impact strength, (c) desirability optimization for flexural strength.

3.2. Analysis by Machine Learning Using a Nonlinear Regressor

A mathematical model for predicting flexural strength, tensile strength, and impact strength was developed using nonlinear regression in MATLAB R2020a. In the equations, x_1 , x_2 , x_3 , and x_4 denote the infill percentage, layer height, print speed, and extrusion temperature, respectively, where, y_1 , y_2 , and y_3 denote the corresponding tensile strength, impact strength, and flexural strength, respectively.

Tensile strength

$$y_1 = 61.977 + 0.66315x_1 + 168.67x_2 + 0.696x_3 - 0.7408x_4 - 0.40833x_1 x_2 + 0.00020741x_1 x_3 - 0.0023722 x_1 x_4 + 0.54583x_2 x_3 - 0.44219x_2 x_4 - 0.0037083x_3 x_4 + 0.00039318x_1^2 - 193.12x_2^2 - 0.00073201x_3^2 + 0.002903x_4^2 \quad (1)$$

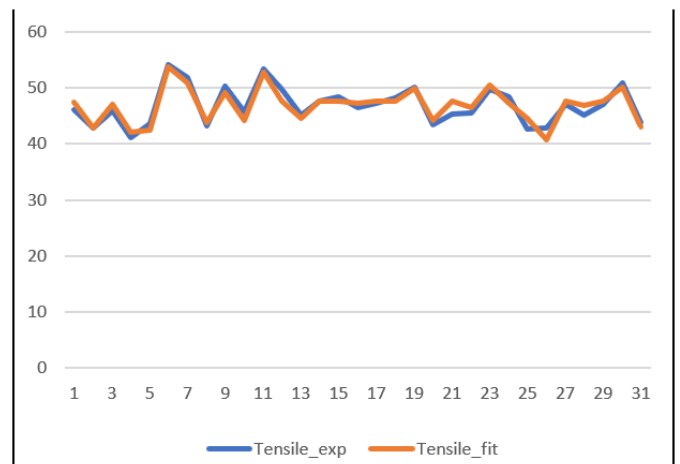
Impact strength

$$y_2 = -71.12 + 0.1587x_1 + 23.889x_2 - 0.21128x_3 + 0.71328x_4 - 0.0625x_1 x_2 + 0.00027037x_1 x_3 - 0.00053889 x_1 x_4 + 0.082292x_2 x_3 - 0.12656x_2 x_4 + 0.00073333x_3 x_4 - 0.00036484x_1^2 + 1.9996x_2^2 + 0.00025688x_3^2 - 0.001697x_4^2 \quad (2)$$

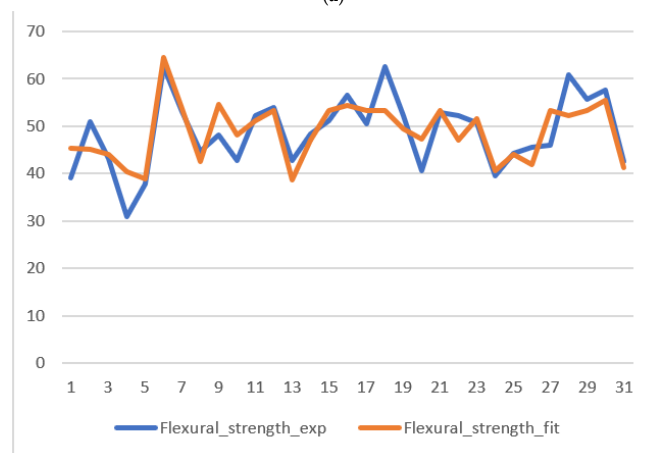
Flexural strength

$$y_3 = -540 + 1.399 x_1 + 426.71x_2 - 1.3823 x_3 + 5.3741 x_4 - 0.063194 x_1 x_2 + 0.00027037x_1 x_3 - 0.0057389x_1 x_4 + 0.95833x_2 x_3 - 1.3531x_2 x_4 + 0.010917x_3 x_4 + 0.00073792x_1^2 - 403.93x_2^2 - 0.010451x_3^2 - 0.012427x_4^2 \quad (3)$$

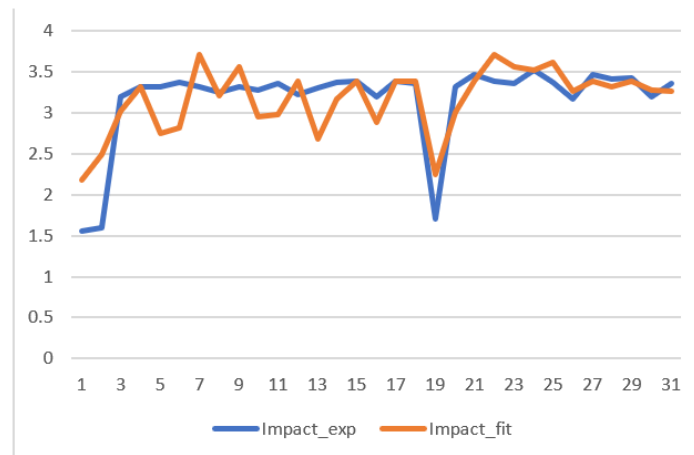
The plots of experimental versus predicted values are shown below in Figure 7. The graphs show that the tensile strength and flexural strength model achieve a minimum error. The optimum values were obtained using MATLAB R2020a on Windows Platform with Intel Core i7 with 8GB RAM. The optimum values were obtained for all of the outputs. The infill percentage, layer height, print speed, and extrusion temperature should be 100%, 0.0962 mm, 20 mm/s, and 230 °C, respectively, to obtain the optimum tensile strength. The optimum impact strength can be obtained if the infill percentage, layer height, print speed, and extrusion temperature are 70%, 0.08 mm, 20 mm/s, and 201 °C, respectively. To obtain the optimum flexural strength, the infill percentage, layer height, print speed, and extrusion temperature should be set at 100%, 0.24 mm, 52 mm/s, and 203 °C, respectively.



(a)



(b)



(c)

Figure 7. (a) Tensile strength between nonlinear regression and experimental, (b) flexural strength between nonlinear regression and experimental, (c) impact strength between nonlinear regression and experimental.

3.3. Comparison of Results

Validation experiments were carried out to verify the predicted output parameters as FDM-processed parts are again fabricated using these parameter settings, and all tensile, impact, and flexural test were carried out to validate the obtained results, as depicted in Table 3.

Table 3. Validation experiments.

Responses (Output Parameter)	Desirability Approach	Nonlinear Regression	Experimental	Error (%) Desirability Approach	Error (%) Nonlinear Regression
Tensile Strength (N/mm ²)	59.6875	59.6069	57.832	3.109	2.977
Impact Strength (kJ/m ²)	4.3020	4.3020	4.021	6.532	6.532
Flexural Strength (N/mm ²)	65.3043	65.1432	62.88	3.712	3.474

The desirability approach, nonlinear regression, as well as experimental values are much closer to each other, which validates the desirability approach, and the process parameter settings obtained with nonlinear regression will achieve the optimum values of flexural strength, tensile strength, and impact strength.

4. Conclusions

In this study, two approaches are implemented to understand the effect of process parameters on mechanical properties. The first one is based on design of experiments, i.e., the central composite design of response surface methodology. A total of 31 runs were carried out. The desirability concept was used to optimize the tensile strength, impact strength, and flexural strength by obtaining the optimal settings of input process parameters, namely, infill percentage, layer height, print speed, and extrusion temperature. Secondly, the non-linear regression method was employed to predict the tensile strength, impact strength, and flexural strength. Further, the optimal input parameter settings were also obtained based on non-linear regression. The key finds are as follows:

1. It was found that the infill percentage has a maximum effect on tensile strength and flexural strength, while extrusion temperature has a maximum effect on impact strength.
2. Mathematical models for tensile strength, impact strength, and flexural strength were developed using nonlinear regression.
3. Eventually, optimum values of tensile strength, impact strength, and flexural strength were found using the desirability approach and nonlinear regression and were validated experimentally.
4. The desirability approach predicts the tensile strength, impact strength, and flexural strength with a percentage error of less than 3.109, 6.532, and 3.712, respectively.
5. The nonlinear regression approach predicts the tensile strength, impact strength, and flexural strength with a percentage error of less than 2.977, 6.532, and 3.474, respectively.

The future scope of this study is to work upon improvements in shear strength, fatigue strength, surface properties, and dimensional accuracy of the parts printed using PLA and, furthermore, to use a machine learning regressor and classifier for the prediction of mechanical properties, surface properties, and dimensional accuracy.

Author Contributions: Conceptualization, V.S.J. (Vijaykumar S. Jatti); methodology, V.S.J. (Vijaykumar S. Jatti); software, V.S.J. (Vijaykumar S. Jatti); validation, M.S.S.; formal analysis, M.S.S.; investigation, M.S.S.; resources, V.S.J. (Vijaykumar S. Jatti); data curation, N.K.K.; writing—original draft preparation, V.S.J. (Vijaykumar S. Jatti); writing—review and editing, A.V.J.; visualization, V.S.J. (Vijaykumar S. Jatti); supervision, A.V.J.; project administration, N.K.K. All authors have read and agreed to the published version of the manuscript.

Funding: This research received no external funding.

Institutional Review Board Statement: Not applicable.

Informed Consent Statement: Not applicable.

Data Availability Statement: Not applicable.

Acknowledgments: Thanks to the college administration for supporting this work. Symbiosis Institute of Technology has supported for paying the open access fee.

Conflicts of Interest: The authors declare no conflict of interest.

References

- Masood, S.H. Advances in fused deposition modelling. *Compr. Mater. Process.* **2014**, *10*, 69–91. [\[CrossRef\]](#)
- Dudescu, C.; Racz, L. Effects of raster orientation, infill rate and infill pattern on the mechanical properties of 3D printed materials. *ACTA Universitatis Cibiniensis Tech. Ser.* **2017**, *69*, 23–30. [\[CrossRef\]](#)
- Fernandes, J.; Deus, A.M.; Reis, L.; Vaz, M.F.; Leite, M. Study of the influence of 3D printing parameters on the mechanical properties of PLA. In Proceedings of the 3rd International Conference on Progress in Additive Manufacturing (Pro-AM 2018), Singapore, 14–17 May 2018; pp. 547–552. [\[CrossRef\]](#)
- Bähr, F.; Westkämper, E. Correlations between influencing parameters and quality properties of components produced by fused deposition modeling. *Procedia Cirp.* **2018**, *72*, 1214–1219. [\[CrossRef\]](#)
- Kantaros, A.; Karalekas, D. Fiber Bragg grating based investigation of residual strains in ABS parts fabricated by fused deposition modeling process. *Mater. Des.* **2013**, *50*, 44–50. [\[CrossRef\]](#)
- Sood, A.K.; Ohdar, R.K.; Mahapatra, S.S. Improving dimensional accuracy of Fused Deposition Modelling processed part using grey Taguchi method. *Mater. Des.* **2009**, *30*, 4243–4252. [\[CrossRef\]](#)
- Sood, A.K.; Ohdar, R.K.; Mahapatra, S.S. Parametric appraisal of mechanical property of fused deposition modelling processed parts. *Mater. Des.* **2010**, *31*, 287–295. [\[CrossRef\]](#)
- Es-Said, O.S.; Foyos, J.; Noorani, R.; Mendelson, M.; Marloth, R.; Pregger, B.A. Effect of Layer Orientation on Mechanical Properties of Rapid Prototyped Samples. *Mater. Manuf. Process.* **2007**, *15*, 107–122. [\[CrossRef\]](#)
- Kantaros, A.; Karalekas, D. Employing a Low-Cost Desktop 3D Printer: Challenges, and How to Overcome Them by Tuning Key Process Parameters. *Int. J. Mech. Appl.* **2021**, *10*, 11–19. [\[CrossRef\]](#)
- Vasudevarao, B.; Natarajan, D.P.; Henderson, M.; Razdan, A. Sensitivity of rp surface finish to process parameter variation. *Int. Solid Free. Fabr. Symp.* **2000**, *1*, 251–258. [\[CrossRef\]](#)
- Kantaros, A.; Karalekas, D. FBG Based In Situ Characterization of Residual Strains in FDM Process. In *Residual Stress, Thermo-mechanics & Infrared Imaging, Hybrid Techniques and Inverse Problems*; Conference Proceedings of the Society for Experimental Mechanics Series; Springer: Cham, Switzerland, 2014; Volume 8, p. 8. [\[CrossRef\]](#)
- Tran, N.H.; Nguyen, V.N.; Ngo, A.V.; Nguyen, V.C. Study on the effect of fused deposition modeling (FDM) process parameters on the printed part quality. *Int. J. Eng. Res. Appl.* **2017**, *7*, 71–77. [\[CrossRef\]](#)
- Popescu, D.; Zapciu, A.; Amza, C.; Baciuc, F.; Marinescu, R. FDM process parameters influence over the mechanical properties of polymer specimens: A review. *Polym. Test.* **2018**, *69*, 157–166. [\[CrossRef\]](#)
- Ding, S.; Zou, B.; Wang, P.; Ding, H. Effects of nozzle temperature and building orientation on mechanical properties and microstructure of PEEK and PEI printed by 3D-FDM. *Polym. Test.* **2019**, *78*, 105948. [\[CrossRef\]](#)
- Peng, A.; Xiao, X.; Yue, R. Process parameter optimization for fused deposition modeling using response surface methodology combined with fuzzy inference system. *Int. J. Adv. Manuf. Technol.* **2014**, *73*, 87–100. [\[CrossRef\]](#)
- Zhang, J.W.; Peng, A.H. Process-parameter optimization for fused deposition modeling based on Taguchi method. *Adv. Mater. Res.* **2012**, *538*, 444–447. [\[CrossRef\]](#)
- Gao, G.; Xu, F.; Xu, J.; Tang, G.; Liu, Z. A Survey of the Influence of Process Parameters on Mechanical Properties of Fused Deposition Modeling Parts. *Micromachines* **2022**, *13*, 553. [\[CrossRef\]](#) [\[PubMed\]](#)
- Alhazmi, M.W.; Backar, A.; Backar, A.H. Influence of infill density and orientation on the mechanical response of PLA+ specimens produced using FDM 3D printing. *Int. J. Adv. Sci. Technol.* **2020**, *29*, 3362–3371.
- Ayatollahi, M.R.; Nabavi-Kivi, A.; Bahrami, B.; Yahya, M.Y.; Khosravani, M.R. The influence of in-plane raster angle on tensile and fracture strengths of 3D-printed PLA specimens. *Eng. Fract. Mech.* **2020**, *237*, 107225. [\[CrossRef\]](#)
- Banerjee, D.; Mishra, S.B.; Khan, M.S.S.; Ajay Kumar, M.A. Mathematical approach for the geometrical deformation of fused deposition modelling build parts. *Mater. Today Proc.* **2020**, *33*, 5051–5054. [\[CrossRef\]](#)
- Dave, H.K.; Prajapati, A.R.; Rajpurohit, S.R.; Patadiya, N.H.; Raval, H.K. Investigation on tensile strength and failure modes of FDM printed part using in-house fabricated PLA filament. *Adv. Mater. Process. Technol.* **2020**. [\[CrossRef\]](#)
- Deshwal, S.; Kumar, A.; Chhabra, D. Exercising hybrid statistical tools GA-RSM, GA-ANN and GA-ANFIS to optimize FDM process parameters for tensile strength improvement. *CIRP J. Manuf. Sci. Technol.* **2020**, *31*, 189–199. [\[CrossRef\]](#)
- Heidari-Rarani, M.; Ezati, N.; Sadeghi, P.; Badrossamay, M.R. Optimization of FDM process parameters for tensile properties of polylactic acid specimens using Taguchi design of experiment method. *J. Thermoplast. Compos. Mater.* **2020**, *2020*, 560. [\[CrossRef\]](#)
- Omiyale, P.K.; Omiyale, B.O. Mechanical behaviour of polylactic acid parts fabricated via material extrusion process: A taguchi-grey relational analysis approach. *Int. J. Eng. Res. Afr.* **2020**, *46*, 32–44.
- Fountas, N.A.; Kostazos, P.; Pavlidis, H.; Antoniou, V.; Manolagos, D.E.; Vaxevanidis, N.M. Experimental investigation and statistical modelling for assessing the tensile properties of FDM fabricated parts. *Procedia Struct. Integr.* **2020**, *26*, 139–146. [\[CrossRef\]](#)

26. Srinivasu, K.K.; Srinivasu, G. Effect of post treatment on tensile properties of carbon reinforced PLA composite by 3D printing. *Mater. Today Proc.* **2020**, *33*, 5403–5407.
27. Gunasekaran, K.N.; Aravinth, V.; Kumaran, C.B.M.; Madhankumar, K.; Pradeep Kumar, S. Investigation of mechanical properties of PLA printed materials under varying infill density. *Mater. Today Proc.* **2020**, *45*, 1849–1856. [[CrossRef](#)]
28. Kamaal, M.; Anas, M.; Rastogi, H.; Bhardwaj, N.; Rahaman, A. Effect of FDM process parameters on mechanical properties of 3D-printed carbon fibre-PLA composite. *Prog. Addit. Manuf.* **2021**, *6*, 63–69. [[CrossRef](#)]
29. Kozior, T.; Mamun, A.; Trabelsi, M.; Sabantina, L.; Ehrmann, A. Quality of the surface texture and mechanical properties of FDM printed samples after thermal and chemical treatment. *Stroj. Vestn. J. Mech. Eng.* **2020**, *66*, 105–113.
30. Kumar, M.A.; Khan, M.S.; Mishra, S.B. Effect of fused deposition machine parameters on tensile strength of printed carbon fiber reinforced pla thermoplastics. *Mater. Today Proc.* **2020**, *27*, 1505–1510. [[CrossRef](#)]
31. Lee, D.; Wu, G.Y. Parameters affecting the mechanical properties of three-dimensional (3D) printed carbon fiberreinforced polylactide composites. *Polymers* **2020**, *12*, 2456. [[CrossRef](#)]
32. Blessie, J. Optimization of process parameters for improving mechanical strength of pla plastics using Taguchi method. *Int. Res. J. Eng. Technol.* **2020**, *35*, 6264–6268.
33. Son, T.A.; Minh, P.S.; Thanh, T.D. Effect of 3D printing parameters on the tensile strength of products. *Key Eng. Mater.* **2020**, *863*, 103–108. [[CrossRef](#)]
34. Tang, C.; Liu, J.; Yang, Y.; Liu, Y.; Jiang, S.; Hao, W. Effect of process parameters on mechanical properties of 3D printed PLA lattice structures. *Compos. Part C Open Access* **2020**, *3*, 100076. [[CrossRef](#)]
35. Vălean, C.; Marsavina, L.; Mărghitas, M.; Linul, E.; Razavi, J.; Berto, F. Effect of manufacturing parameters on tensile properties of FDM printed specimens. *Procedia Struct. Integr.* **2020**, *26*, 313–320. [[CrossRef](#)]
36. Vardhan, H.; Kumar, R.; Chohan, J.S. Investigation of tensile properties of sprayed aluminium based PLA composites fabricated by FDM technology. *Mater. Today Proc.* **2020**, *33*, 1599–1604. [[CrossRef](#)]
37. Waseem, M. Multi-response optimization of tensile creep behavior of PLA 3D printed parts using categorical response surface methodology. *Polymers* **2020**, *12*, 2962. [[CrossRef](#)]
38. Yao, T.; Ye, J.; Deng, Z.; Zhang, K.; Ma, Y.; Ouyang, H. Tensile failure strength and separation angle of FDM 3D printing PLA material: Experimental and theoretical analyses. *Compos. Part B Eng.* **2020**, *188*, 107894. [[CrossRef](#)]
39. Zandi, M.D.; Jerez-Mesa, R.; Lluma-Fuentes, J.; Jorba-Peiro, J.; Travieso-Rodríguez, J.A. Study of the manufacturing process effects of fused filament fabrication and injection molding on tensile properties of composite PLA-wood parts. *Int. J. Adv. Manuf. Technol.* **2020**, *108*, 1725–1735. [[CrossRef](#)]
40. Algarni, M. The influence of raster angle and moisture content on the mechanical properties of pla parts produced by fused deposition modeling. *Polymers* **2021**, *13*, 237. [[CrossRef](#)]
41. Dou, H.; Cheng, Y.; Ye, W.; Zhang, D.; Li, J.; Miao, Z.; Rudykh, S. Effect of process parameters on tensile mechanical properties of 3D printing continuous carbon fiber-reinforced PLA composites. *Materials* **2020**, *13*, 3850. [[CrossRef](#)]
42. Reverte, J.M.; Caminero, M.Á.; Chacón, J.M.; García-Plaza, E.; Núñez, P.J.; Becar, J.P. Mechanical and geometric performance of PLA-based polymer composites processed by the fused filament fabrication additive manufacturing technique. *Materials* **2020**, *13*, 1924. [[CrossRef](#)]
43. Mustafa, M.S.; Zafar, M.Q.; Muneer, M.A.; Arif, M.; Siddiqui, F.A.; Javed, H.M.A. Process parameter optimization in fused deposition modeling using response surface methodology. *Res. Sq.* **2020**, *19*. [[CrossRef](#)]
44. Awasthi, P.; Banerjee, S.S. Fused deposition modeling of thermoplastic elastomeric materials: Challenges and opportunities. *Addit. Manuf.* **2021**, *46*, 102177. [[CrossRef](#)]
45. Cuan-Urquizo, E.; Barocio, E.; Tejada-Ortigoza, V.; Pipes, R.B.; Rodriguez, C.A.; Roman-Flores, A. Characterization of the Mechanical Properties of FFF Structures and Materials: A Review on the Experimental, Computational and Theoretical Approaches. *Materials* **2019**, *12*, 895. [[CrossRef](#)] [[PubMed](#)]
46. Verma, N.; Aiswarya, S.; Banerjee, S.S. Development of material extrusion 3D printable ABS/PC polymer blends: Influence of styrene–isoprene–styrene copolymer on printability and mechanical properties. *Polym. Plast. Technol. Mater.* **2022**, *2022*, 218. [[CrossRef](#)]